Current Biology 21, 574–579, April 12, 2011 ©2011 Elsevier Ltd All rights reserved DOI 10.1016/j.cub.2011.02.034

Report

Decoupling of Activation and Effector Binding Underlies ARF6 Priming of Fast Endocytic Recycling

Guillaume Montagnac,[1,2,*] Hélène de Forges,[1,2] Elizabeth Smythe,[6] Charles Gueudry,[3,7] Maryse Romao,[1,5] Jean Salamero,[1,3,4] and Philippe Chavrier[1,2,*]
[1]Centre de Recherche, Institut Curie
[2]Membrane and Cytoskeleton Dynamics
[3]Plateforme d'Imagerie Cellulaire et Tissulaire-Infrastructures en Biologie Santé et Agronomie (PICT-IBiSA)
[4]Molecular Mechanisms of Intracellular Transport
[5]Structure and Membrane Compartments
CNRS, UMR 144, 26 rue d'Ulm, 75248 Paris Cedex 05, France
[6]Department of Biomedical Science, University of Sheffield, Sheffield S10 2TN, UK
[7]Roper Scientific SAS, 8 rue du Forez, 91017 Evry Cedex, France

Summary

The small GTP-binding protein ADP-ribosylation factor 6 (ARF6) controls the endocytic recycling pathway of several plasma membrane receptors. We analyzed the localization and GDP/GTP cycle of GFP-tagged ARF6 by total internal reflection fluorescent microscopy. We found that ARF6-GFP associates with clathrin-coated pits (CCPs) at the plasma membrane in a GTP-dependent manner in a mechanism requiring the adaptor protein complex AP-2. In CCP, GTP-ARF6 mediates the recruitment of the ARF-binding domain of downstream effectors including JNK-interacting proteins 3 and 4 (JIP3 and JIP4) after the burst recruitment of the clathrin uncoating component auxilin. ARF6 does not contribute to receptor-mediated clathrin-dependent endocytosis. In contrast, we found that interaction of ARF6 and JIPs on endocytic vesicles is required for trafficking of the transferrin receptor in the fast, microtubule-dependent endocytic recycling pathway. Our findings unravel a novel mechanism of separation of ARF6 activation and effector function, ensuring that fast recycling may be determined at the level of receptor incorporation into CCPs.

Results and Discussion

ADP-ribosylation factor 6 (ARF6) activity impinges on cellular functions such as cytokinesis, phagocytosis, cell migration, and tumor cell invasion, which have in common a requirement for polarized insertion of plasma membrane (PM) proteins and lipids ([1] and references herein). Several lines of evidence indicate that ARF6 can affect endocytic recycling of receptors, which are internalized via both the clathrin-dependent and -independent routes [2–7]. Guanine-nucleotide exchange factors (GEFs), which catalyze the activation of ARF6 by GTP loading, are generally found at the PM, and it is thus believed that ARF6 activation is restricted to this location, although ARF6 is also present on internal endosomal compartments [8, 9]. Here we studied the mechanism through which plasma membrane GTP-ARF6 regulates endocytic recycling.

When expressed in HeLa cells in fusion with a carboxy-terminal EGFP moiety and visualized by simultaneous two-color total internal reflection fluorescent microscopy (TIRF-M), ARF6-GFP accumulated in punctuate structures, most of them persisting over several minutes of the time-lapse sequence (Figure 1A and Figure 3A; see also Movie S1 available online). ARF6-GFP accumulations were positive for clathrin light chain (mRFP-LCa; Figure 1A and Figure 3A) and clathrin-adaptor protein complex AP-2 (Figure S1A), identifying ARF6-GFP puncta as clathrin-coated structures (CCSs). TIRF-M analysis of ARF6-GFP in HeLa cells revealed no association with caveolin-1 puncta (see Figure S1B), nor did GFP alone associate with CCSs (Figure S1C). In HeLa cells, CCSs, also referred to as clathrin-coated plaques, are long-lived structures competent for endocytosis [10, 11]. As described previously, BSC1 cells showed dynamically assembling and disappearing clathrin-coated pits (CCPs) [12], which were similarly positive for ARF6-GFP (Figure 3B).

We compared the distribution of ARF6-GFP with that of the widely used ARF6-HA construct by cell fractionation, and we observed a similar membrane association of both constructs, as well as some cytosolic accumulation, whereas endogenous ARF6 was predominantly membrane associated, as reported [13, 14] (Figure S1D). In addition, ARF6-GFP and ARF6-HA were activated (i.e., loaded with GTP) to similar levels in response to the ARF6-specific GEF, EFA6 [15] (3.7-fold ± 1.3-fold increase of GTP-bound ARF6-HA as compared to 2.8-fold ± 0.3-fold for ARF6-GFP; see Figure S1E), supporting the use of ARF6-GFP as a bona fide ARF6 mimic. We also observed that an internally GFP-tagged ARF6 construct previously described to match the properties of endogenous ARF6 [14] similarly accumulated in CCSs in HeLa cells, ruling out some positioning effect of the tag on ARF6-GFP localization (Figure S1F). Furthermore, we found that endogenous ARF6 was enriched in a purified clathrin-coated vesicle fraction to greater extent than Rab5, another small GTPase associated with CCVs [16] (Figure 1B). Finally, localization of ARF6-GFP and ARF6-HA by cryoimmunogold electron microscopy revealed an association with plasma membrane invagination and vesicles in the vicinity of the plasma membrane (Figures S1G and S1H). Altogether, these observations identify ARF6 as a new component of CCP and CCSs.

Interplay of ARF6 and AP-2 at the PM has been reported [5, 6], and it was suggested that the recruitment of AP-2 at the PM might be under ARF6 control through a direct interaction of GTP-ARF6 with AP-2 [6]. However, knocking down the expression of ARF6 did not cause significant reduction of PM association of clathrin or of AP-2 into CCPs in HeLa cells (Figure 1C; see also Figures S1I–S1L). In contrast, when we knocked down AP-2 μ2 or α subunits, leading to the expected drastic reduction in CCSs, the PM accumulation of ARF6-GFP was completely abolished, including in CCSs that persisted in AP-2-depleted cells (Figures 1D and 1E and Figures S1M and S1N). Thus, we conclude that AP-2 is required for PM accumulation of ARF6-GFP in CCSs. Finally, clathrin heavy chain depletion did not affect PM accumulation of AP-2, as

*Correspondence: guillaume.montagnac@curie.fr (G.M.), philippe.chavrier@curie.fr (P.C.)

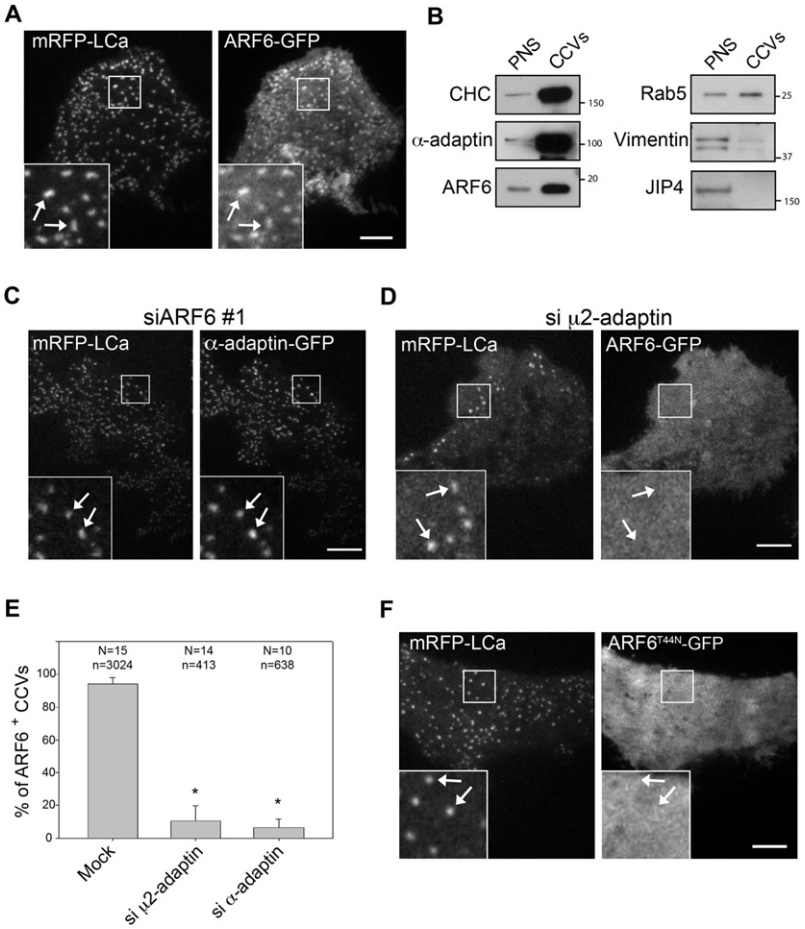

Figure 1. ARF6 Localizes to Plasma Membrane Clathrin-Coated Structures

(A) HeLa cells overexpressing wild-type ARF6-GFP and mRFP-LCa (clathrin light chain) were imaged by two-color total internal reflection fluorescent microscopy (TIRF-M). Higher magnifications of boxed areas are shown. Arrows point to clathrin-coated structures (CCSs).

(B) Postnuclear supernatant (PNS) and clathrin-coated vesicle (CCV) fractions (10 μg) isolated from porcine brain were analyzed by SDS-PAGE followed by immunoblotting with indicated antibodies. Data are representative of two independent fractionation experiments. Molecular weights are indicated in kDa.

(C) HeLa cells treated with ARF6 small interfering RNA (siRNA) were transfected with mRFP-LCa and α-adaptin-GFP constructs and observed by TIRF-M. Higher magnification of boxed areas is shown in insets. Arrows point to CCSs.

(D) μ2-adaptin-depleted HeLa cells were transfected with mRFP-LCa and ARF6-GFP constructs and imaged by TIRF-M. Higher magnification of boxed areas is shown in insets. Arrows point to remaining CCSs.

(E) Quantification of the percentage of CCSs (identified by mRFP-LCa) positive for ARF6-GFP in control cells or cells depleted for AP-2 μ2 or α-adaptin subunit. N denotes number of cells analyzed; n denotes number of CCSs analyzed; *p < 0.001 compared to mock-treated cells.

(F) HeLa cells overexpressing GDP-bound ARF6^{T44N}-GFP and mRFP-LCa were imaged by two-color TIRF-M. Higher magnifications of boxed areas are shown. Arrows point to CCSs. Scale bars represent 5 μm.

previously described [17], or that of ARF6-GFP that colocalized with AP-2 (Figure S1O), indicating that clathrin does not control the recruitment of ARF6 into CCSs.

Mutant forms of ARF6 with impaired binding to GTP (GDP-locked ARF6^{T44N}-GFP) or to both GDP and GTP (nucleotide-free ARF6^{T27N}-GFP) [18] did not associate with CCSs (Figure 1F and data not shown), suggesting that ARF6-GFP localization to CCSs requires GTP loading. In contrast, a fast-cycling mutant of ARF6 (ARF6^{T157N}-GFP [19, 20]) and a mutant unable to hydrolyze GTP (ARF6^{Q67L}-GFP) both localized to CCSs (see Movie S2 and data not shown). We used two-color fluorescent recovery after photobleaching (FRAP) by TIRF-M to monitor the kinetics of association and dissociation of ARF6-GFP and mRFP-LCa to individual CCS in HeLa cells and their regulation by GTP binding and hydrolysis on ARF6. During FRAP, exchange of bleached wild-type ARF6-GFP in CCSs with unbleached ARF6-GFP was almost complete (mean intensity recovery of ~94%) and relatively fast with a half-time of recovery ($t_{1/2}$) of ~9 s (Figure 2 and Movie S2). Recovery of ARF6^{T157N}-GFP was faster than wild-type ($t_{1/2}$ = ~2.5 s; Figure 2). Because this mutant is predominantly in the active GTP-bound conformation as a result of the higher concentration of GTP versus GDP in cytosol [19, 20], this result further emphasizes the importance of GTP loading for incorporation of ARF6-GFP in CCSs. In contrast, recovery of constitutively activated ARF6^{Q67L}-GFP was slower ($t_{1/2}$ = ~16 s) and reached a plateau at ~60% of prebleach fluorescence, indicating that GTP hydrolysis is required for normal dynamics of ARF6 in CCSs (Figure 2 and Movie S2). Two-color FRAP allowed simultaneous analysis of recovery kinetics of clathrin light chain, revealing that expression of wild-type or mutant ARF6 did not significantly affect the dynamics of clathrin light chain in CCSs (Figure 2B, italics, and Movie S2). Altogether, these data indicate that GTP loading and GTP hydrolysis are required for ARF6 incorporation and dynamics in CCSs, suggesting essential roles for one or more yet-unknown ARF6-specific GEFs and GAPs.

Kymograph analysis of TIRF-M time-lapse sequences confirmed that ARF6-GFP is present along the entire lifespan of persistent CCSs in HeLa cells (Figure 3A) and in rapidly assembling and disassembling CCPs in BSC1 cells (Figure 3B). The ARF-binding domain (ABD) of the ARF6-specific effector JIP3 (JIP3^{ABD}), which can detect GTP-bound ARF6 in biochemical assays [21, 22], was then used to localize activated ARF6 in BSC1 cells. In contrast to ARF6-GFP, GFP-JIP3^{ABD} showed a transient association with some CCPs (Figure 3C). Analysis of disappearing mRFP-LCa CCPs revealed that 36.5% ended with a burst of GFP-JIP3^{ABD} signal (Figure 3E and Movie S3). This fraction dropped to 11.7% in cells coexpressing the dominant-negative ARF6^{T27N} mutant (Figure 3E), demonstrating that recruitment of GFP-JIP3^{ABD} to CCPs requires activation of endogenous ARF6. A burst of association coinciding with CCP disappearance is the hallmark of components of the vesicle-uncoating reaction, including auxilin and cyclin G-associated kinase (GAK), which recruit Hsc70 to assembled clathrin and disrupt clathrin-clathrin

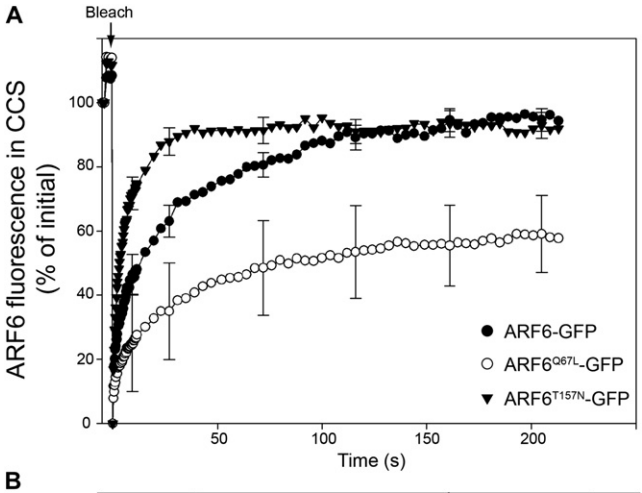

B

	Mean Intensity Recovery (%)	Mean $t_{1/2}$ (s)	n
ARF6 *(LCa)*	94.4 +/- 8.9 *(84.7 +/- 12.7)*	8.9 +/- 3.7 *(5.7 +/- 1.7)*	34
$ARF6^{Q67L}$ *(LCa)*	58.3 +/- 13.4 * *(69.4 +/- 15.2)*	16.1 +/- 15.2 * *(4.3 +/- 2.7)*	24
$ARF6^{T157N}$ *(LCa)*	92.6 +/- 10.7 *(81.3 +/- 11)*	2.5 +/- 1.2 * *(5.8 +/- 2.2)*	28

Figure 2. GDP/GTP Cycle Controls the Dynamics of ARF6-GFP in CCSs

Kinetics of association and dissociation of ARF6-GFP mutants and mRFP-LCa to individual CCS in HeLa cells measured by two-color fluorescent recovery after photobleaching (FRAP).

(A) Average FRAP curves for wild-type and mutant ARF6-GFP.

(B) FRAP parameters (mean intensity recovery and half-life [$t_{1/2}$]) for ARF6-GFP and mRFP-LCa (italics) calculated from the indicated numbers (n) of CCSs from three independent experiments. Error bars indicate the standard deviations; *$p < 0.001$ compared to ARF6-GFP-expressing cells.

interactions [23–25]. Similarly to a previous report [25], we observed that ~58% of LCa-positive CCPs presented a burst of GFP-auxilin at the time of disassembly (Figure 3E). Some auxilin-negative CCPs (~42%) may correspond to abortive structures that disassembled before reaching maturity [12, 25–27]. Remarkably, the fraction of CCPs ending with a burst of auxilin remained unchanged in cells expressing $ARF6^{T27N}$ (Figure 3E), indicating that GTP-ARF6 does not significantly contribute to auxilin recruitment. The smaller fraction of CCPs ending with a burst of JIP3 as compared to auxilin-ending ones may suggest that only a subset of CCPs contains significant levels of GTP-ARF6 to support JIP3 recruitment.

The use of simultaneous two-color TIRF-M allowed direct comparison of the timing of recruitment of $JIP3^{ABD}$ relative to that of auxilin. We found that the burst of auxilin consistently occurred shortly before the recruitment of $JIP3^{ABD}$ in both BSC1 and HeLa cells (Figure 3D and Figure S2A). Similarly, the burst of auxilin preceded that of the ARF-binding domain of ARHGAP21, an ARF effector protein that can interact with all ARF family members in their GTP-bound state [28, 29] (see Figure S2B). On average, the burst of $JIP3^{ABD}$ occurred 1.2 ± 0.8 s after initial detection of auxilin fluorescence (Figure 3D). Importantly, TIRF-M also revealed that endocytic vesicles labeled with Alexa Fluor 488 transferrin (Tf) rapidly disappeared from the evanescent field, as indicated by signal of the cargo that quickly vanished after the loss of LCa fluorescence (1.6 ± 2.1 s; see Figure S2C). This is similar to the disappearance of $JIP3^{ABD}$ fluorescence following loss of auxilin signal (2.0 ± 2.1 s; see Figure S2D), indicating that Tf/ARF6/JIP-positive endocytic vesicles rapidly moved away from the PM after they underwent fission and uncoating. Along this line, when we looked at the cytoplasmic distribution of ARF6-GFP by confocal spinning disk microscopy of HeLa cells labeled with Alexa 546-conjugated Tf, ARF6-GFP was present on numerous highly dynamic Tf-positive endocytic vesicles and endosomes, in agreement with previous ultrastructural investigations [8, 13] (see Movie S4). Of note, ARF6-GFP was also present on large, poorly dynamic Tf-negative vacuolar structures (see Movie S4) that might be related to bulk plasma membrane endocytosis or to a described role of ARF6 in a clathrin-independent endocytic recycling pathway [3, 7].

Altogether, these data suggest that GTP-ARF6 is present in a subset of CCS and CCPs and becomes accessible to downstream effectors only after vesicle uncoating. This argues that ARF6 activation and incorporation in CCPs is dissociated in time and space from effector binding and function. This subset of GTP-ARF6 CCPs may be defined by incorporation of specific receptors able to trigger ARF6 activation upon engagement. Recent work has demonstrated that a large conformational change of AP-2 that allows strong membrane attachment and cargo binding is driven by $PtdIns4,5P_2$, probably with no contribution of ARF6 ([30] and this study). Together with previous work showing that GTP-ARF6 may interact with AP-2 [6], our data suggest that upon activation, GTP-ARF6 is engaged in effector-like interactions with membrane-bound AP-2 and hence becomes stabilized in CCPs. Therefore, it can be postulated that steric hindrance of GTP-ARF6 in complex with AP-2 is the basis for preventing effector access to ARF6. Hydrolysis of $PtdIns4,5P_2$ [31] and loss of coat components during the uncoating reaction would free membrane-bound GTP-ARF6 and make it available for interaction with its downstream effectors.

We went on analyzing the role of ARF6 in receptor-mediated endocytosis in the clathrin-dependent pathway. ARF6 knockdown or expression of dominant inhibitory $ARF6^{T27N}$-HA did not interfere with the initial rate of Tf endocytosis in HeLa cells ($\leq$5–6 min of Tf uptake; Figure 4A and see Figure S3A), and ARF6 depletion did not affect uptake of EGF (Figure S3B). These observations, indicating no role for ARF6 in clathrin-mediated endocytosis, are in agreement with our assumption that ARF6 is dormant in CCPs and becomes accessible to the effector machinery only after vesicle uncoating, thus after ligand internalization. In contrast, we noticed that whereas intracellular Tf fluorescence dropped rapidly as Tf recycled after the peak of internalization in control cells (the assay measures mainly one cycle of Tf uptake and recycling [32]), interfering with ARF6 function resulted in a significant decrease in Tf recycling (Figure 4A and Figure S3A). This was confirmed with an assay directly measuring Tf recycling (Figure 4B and Figure S3C). Moreover, interfering with ARF6 activity affected mainly the initial phase of recycling ($\leq$8 min of recycling) with a significant ~2-fold decrease of initial Tf recycling rate in ARF6 knocked-down cells as compared to controls (see insets in Figure 4B and Figure S3C). Thus, ARF6 activity is likely to affect primarily a fast-recycling pathway. Therefore, in agreement with seminal findings demonstrating a role of ARF6 in the Tf cycle [2], we conclude that ARF6 controls the fast recycling of Tf following its endocytosis through the clathrin-dependent pathway.

We recently identified two related proteins named JIP3 and JIP4 as new ARF6-specific effectors controlling the trafficking

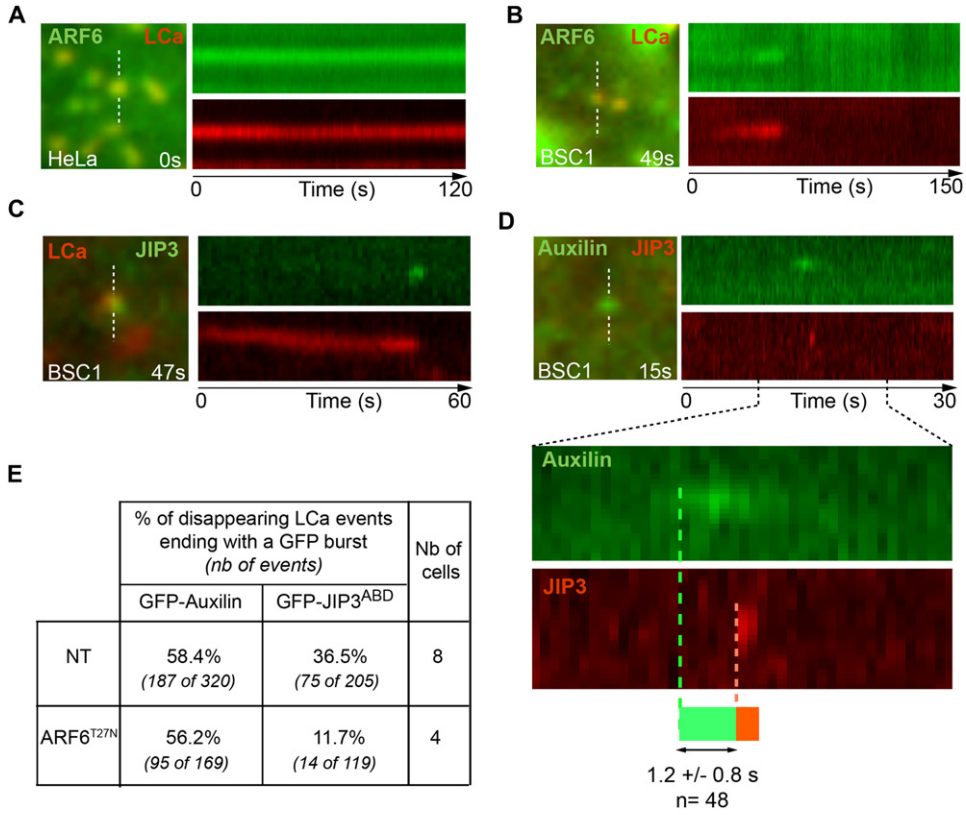

E

	% of disappearing LCa events ending with a GFP burst *(nb of events)*		Nb of cells
	GFP-Auxilin	GFP-JIP3^{ABD}	
NT	58.4% *(187 of 320)*	36.5% *(75 of 205)*	8
ARF6^{T27N}	56.2% *(95 of 169)*	11.7% *(14 of 119)*	4

Figure 3. Vesicle Uncoating Precedes Effector Binding by GTP-ARF6

(A and B) Still images and kymographs of simultaneous two-color TIRF-M time series of HeLa (A) or BSC-1 (B) cells overexpressing ARF6-GFP and mRFP-LCa (1 image/s).

(C) Still images and kymograph views of TIRF time series acquired every second from BSC-1 cells overexpressing GFP-JIP3^{ABD} and mRFP-LCa.

(D) Still images and kymograph views of TIRF time series acquired every 250 ms from BSC-1 cells overexpressing GFP-auxillin and mCherry-JIP3^{ABD}. Enlargement of a portion of kymographs is shown. Average time interval between initial detection of GFP-auxilin and mCherry-JIP3 signals is indicated (n denotes number of CCPs analyzed from ten cells).

(E) Percentage of disappearing mRFP-LCa CCPs ending with a burst of GFP-auxilin or GFP-JIP3^{ABD} in mock- or ARF6^{T27N}-transfected BSC-1 cells. Cell numbers and events analyzed are indicated.

of endosomes along microtubules (MTs). The basis for this new mechanism is the regulation of JIP's interaction with kinesin-1 or dynein/dynactin motors by ARF6: i.e., GTP-ARF6 bound to JIP3/4 favors JIP's association with dynactin while interfering with kinesin-1 binding [21]. In addition, transient association of JIP3^{ABD} in CCPs is consistent with GTP-ARF6 recruiting endogenous JIPs in a subset of CCPs (see Figure 3). Thus, we investigated whether JIP4, the main isoform expressed in HeLa cells [21], may contribute to Tf recycling downstream of ARF6. Similarly to ARF6, knockdown of JIP4 did not affect the kinetics of Tf internalization (data not shown), whereas it impaired initial rates of Tf recycling (compare Figures 4B and 4C and Figure S3D). Moreover, treatment of cells with the MT depolymerizing drug nocodazole also led to similar Tf recycling defects (Figure 4C), indicating that the integrity of the MT network is required for efficient fast recycling of Tf. Interestingly, whereas Tf recycling defects in ARF6-depleted cells could be rescued by expression of a small interfering RNA-resistant form of ARF6, this form harboring mutations impairing binding to JIP3/4 proteins (ARF6^{iSW} [21, 22]) lost the ability to restore normal Tf recycling rates (Figure 4D and Figure S3E). We conclude that interaction of GTP-ARF6 with JIP4 is required for ARF6-dependent fast recycling of Tf in a mechanism also requiring MT integrity.

We showed that upon GTP loading, ARF6 accumulates in CCPs, and vesicle uncoating makes GTP-ARF6 available for recruitment of JIP proteins on endocytic vesicles in a mechanism required for the fast recycling pathway. This unique mechanism of segregation of ARF6 activation and function ensures that fast recycling may be already primed at the level of receptor incorporation into CCPs.

Supplemental Information

Supplemental Information includes three figures, Supplemental Experimental Procedures, and four movies and can be found with this article online at doi:10.1016/j.cub.2011.02.034.

Acknowledgments

We gratefully acknowledge the Nikon Imaging Centre at the Institut Curie-CNRS and the PICT-IBiSA imaging facility of the Institut Curie for help with image acquisition and processing. We are indebted to G. Raposo (Curie Institute, Paris) for help with transmission electron microscopy. We thank T. Kirchhausen, M. Franco, A. Benmerah, C. D'Souza-Schorey, J.H. Keen, and M.A. Schwartz for providing reagents. Support was provided to P.C. by the Association pour la Recherche contre le Cancer, SL220100601356, and the Agence Nationale pour la Recherche, ANR-08-BLAN-0111. Core funding for this work was provided by Institut Curie and CNRS.

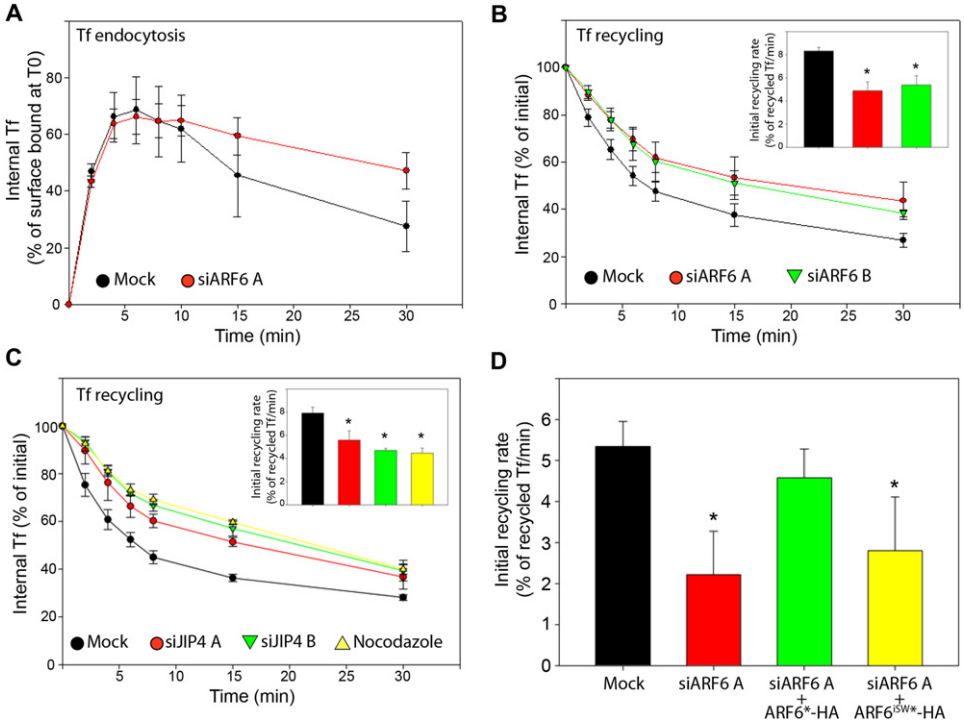

Figure 4. An ARF6 and JIP4 Pathway Controls the Fast Recycling of Tf

(A) HeLa cells were mock treated or treated with ARF6-specific siRNA and assessed for endocytosis of Alexa488-Tf. Data are expressed as percentage of internal Tf compared to surface-bound Tf at time 0 ± standard error of the mean (SEM).

(B) Tf recycling was measured in mock- or siRNA-treated HeLa cells.

(C) HeLa cells were mock treated or treated with JIP4-specific siRNAs or with 10 μM nocodazole and assessed for Tf recycling. In (B) and (C), data are expressed as percentage of internal Tf compared to time 0 ± SEM. Insets in (B) and (C) represent the average rate ± SEM of Tf recycling during the first 8 min of the recycling assay.

(D) HeLa cells were mock treated or treated with siRNA against ARF6 and rescued with siRNA-resistant form of ARF6-HA or ARF6^{iSW}-HA mutant, as indicated, and Tf recycling was assessed. Data are expressed as the average rate ± SEM of Tf recycling during the first 8 min of the assay (*$p < 0.001$ compared to mock-treated cells).

Received: November 23, 2010
Revised: February 7, 2011
Accepted: February 23, 2011
Published online: March 24, 2011

References

1. D'Souza-Schorey, C., and Chavrier, P. (2006). ARF proteins: Roles in membrane traffic and beyond. Nat. Rev. Mol. Cell Biol. *7*, 347–358.
2. D'Souza-Schorey, C., Li, G., Colombo, M.I., and Stahl, P.D. (1995). A regulatory role for ARF6 in receptor-mediated endocytosis. Science *267*, 1175–1178.
3. Radhakrishna, H., and Donaldson, J.G. (1997). ADP-ribosylation factor 6 regulates a novel plasma membrane recycling pathway. J. Cell Biol. *139*, 49–61.
4. Claing, A., Chen, W., Miller, W.E., Vitale, N., Moss, J., Premont, R.T., and Lefkowitz, R.J. (2001). beta-Arrestin-mediated ADP-ribosylation factor 6 activation and beta 2-adrenergic receptor endocytosis. J. Biol. Chem. *276*, 42509–42513.
5. Krauss, M., Kinuta, M., Wenk, M.R., De Camilli, P., Takei, K., and Haucke, V. (2003). ARF6 stimulates clathrin/AP-2 recruitment to synaptic membranes by activating phosphatidylinositol phosphate kinase type Igamma. J. Cell Biol. *162*, 113–124.
6. Paleotti, O., Macia, E., Luton, F., Klein, S., Partisani, M., Chardin, P., Kirchhausen, T., and Franco, M. (2005). The small G-protein Arf6GTP recruits the AP-2 adaptor complex to membranes. J. Biol. Chem. *280*, 21661–21666.
7. Eyster, C.A., Higginson, J.D., Huebner, R., Porat-Shliom, N., Weigert, R., Wu, W.W., Shen, R.F., and Donaldson, J.G. (2009). Discovery of new cargo proteins that enter cells through clathrin-independent endocytosis. Traffic *10*, 590–599.
8. D'Souza-Schorey, C., van Donselaar, E., Hsu, V.W., Yang, C., Stahl, P.D., and Peters, P.J. (1998). ARF6 targets recycling vesicles to the plasma membrane: Insights from an ultrastructural investigation. J. Cell Biol. *140*, 603–616.
9. Casanova, J.E. (2007). Regulation of Arf activation: The Sec7 family of guanine nucleotide exchange factors. Traffic *8*, 1476–1485.
10. Rappoport, J.Z., Kemal, S., Benmerah, A., and Simon, S.M. (2006). Dynamics of clathrin and adaptor proteins during endocytosis. Am. J. Physiol. Cell Physiol. *291*, C1072–C1081.
11. Saffarian, S., Cocucci, E., and Kirchhausen, T. (2009). Distinct dynamics of endocytic clathrin-coated pits and coated plaques. PLoS Biol. *7*, e1000191.
12. Ehrlich, M., Boll, W., Van Oijen, A., Hariharan, R., Chandran, K., Nibert, M.L., and Kirchhausen, T. (2004). Endocytosis by random initiation and stabilization of clathrin-coated pits. Cell *118*, 591–605.
13. Peters, P.J., Hsu, V.W., Ooi, C.E., Finazzi, D., Teal, S.B., Oorschot, V., Donaldson, J.G., and Klausner, R.D. (1995). Overexpression of wild-type and mutant ARF1 and ARF6: Distinct perturbations of nonoverlapping membrane compartments. J. Cell Biol. *128*, 1003–1017.
14. Hall, B., McLean, M.A., Davis, K., Casanova, J.E., Sligar, S.G., and Schwartz, M.A. (2008). A fluorescence resonance energy transfer activation sensor for Arf6. Anal. Biochem. *374*, 243–249.
15. Franco, M., Peters, P.J., Boretto, J., van Donselaar, E., Neri, A., D'Souza-Schorey, C., and Chavrier, P. (1999). EFA6, a sec7 domain-containing exchange factor for ARF6, coordinates membrane recycling and actin cytoskeleton organization. EMBO J. *18*, 1480–1491.
16. Bucci, C., Parton, R.G., Mather, I.H., Stunnenberg, H., Simons, K., Hoflack, B., and Zerial, M. (1992). The small GTPase rab5 functions as a regulatory factor in the early endocytic pathway. Cell *70*, 715–728.

17. Motley, A., Bright, N.A., Seaman, M.N., and Robinson, M.S. (2003). Clathrin-mediated endocytosis in AP-2-depleted cells. J. Cell Biol. *162*, 909–918.
18. Macia, E., Luton, F., Partisani, M., Cherfils, J., Chardin, P., and Franco, M. (2004). The GDP-bound form of Arf6 is located at the plasma membrane. J. Cell Sci. *117*, 2389–2398.
19. Santy, L.C. (2002). Characterization of a fast cycling ADP-ribosylation factor 6 mutant. J. Biol. Chem. *277*, 40185–40188.
20. Klein, S., Franco, M., Chardin, P., and Luton, F. (2006). Role of the Arf6 GDP/GTP cycle and Arf6 GTPase-activating proteins in actin remodeling and intracellular transport. J. Biol. Chem. *281*, 12352–12361.
21. Montagnac, G., Sibarita, J.B., Loubéry, S., Daviet, L., Romao, M., Raposo, G., and Chavrier, P. (2009). ARF6 Interacts with JIP4 to control a motor switch mechanism regulating endosome traffic in cytokinesis. Curr. Biol. *19*, 184–195.
22. Isabet, T., Montagnac, G., Regazzoni, K., Raynal, B., El Khadali, F., England, P., Franco, M., Chavrier, P., Houdusse, A., and Ménétrey, J. (2009). The structural basis of Arf effector specificity: The crystal structure of ARF6 in a complex with JIP4. EMBO J. *28*, 2835–2845.
23. Ungewickell, E., Ungewickell, H., Holstein, S.E., Lindner, R., Prasad, K., Barouch, W., Martin, B., Greene, L.E., and Eisenberg, E. (1995). Role of auxilin in uncoating clathrin-coated vesicles. Nature *378*, 632–635.
24. Massol, R.H., Boll, W., Griffin, A.M., and Kirchhausen, T. (2006). A burst of auxilin recruitment determines the onset of clathrin-coated vesicle uncoating. Proc. Natl. Acad. Sci. USA *103*, 10265–10270.
25. Lee, D.W., Wu, X., Eisenberg, E., and Greene, L.E. (2006). Recruitment dynamics of GAK and auxilin to clathrin-coated pits during endocytosis. J. Cell Sci. *119*, 3502–3512.
26. Mettlen, M., Stoeber, M., Loerke, D., Antonescu, C.N., Danuser, G., and Schmid, S.L. (2009). Endocytic accessory proteins are functionally distinguished by their differential effects on the maturation of clathrin-coated pits. Mol. Biol. Cell *20*, 3251–3260.
27. Loerke, D., Mettlen, M., Yarar, D., Jaqaman, K., Jaqaman, H., Danuser, G., and Schmid, S.L. (2009). Cargo and dynamin regulate clathrin-coated pit maturation. PLoS Biol. *7*, e57.
28. Dubois, T., Paléotti, O., Mironov, A.A., Fraisier, V., Stradal, T.E., De Matteis, M.A., Franco, M., and Chavrier, P. (2005). Golgi-localized GAP for Cdc42 functions downstream of ARF1 to control Arp2/3 complex and F-actin dynamics. Nat. Cell Biol. *7*, 353–364.
29. Ménétrey, J., Perderiset, M., Cicolari, J., Dubois, T., Elkhatib, N., El Khadali, F., Franco, M., Chavrier, P., and Houdusse, A. (2007). Structural basis for ARF1-mediated recruitment of ARHGAP21 to Golgi membranes. EMBO J. *26*, 1953–1962.
30. Jackson, L.P., Kelly, B.T., McCoy, A.J., Gaffry, T., James, L.C., Collins, B.M., Höning, S., Evans, P.R., and Owen, D.J. (2010). A large-scale conformational change couples membrane recruitment to cargo binding in the AP2 clathrin adaptor complex. Cell *141*, 1220–1229.
31. Wenk, M.R., and De Camilli, P. (2004). Protein-lipid interactions and phosphoinositide metabolism in membrane traffic: Insights from vesicle recycling in nerve terminals. Proc. Natl. Acad. Sci. USA *101*, 8262–8269.
32. Dautry-Varsat, A., Ciechanover, A., and Lodish, H.F. (1983). pH and the recycling of transferrin during receptor-mediated endocytosis. Proc. Natl. Acad. Sci. USA *80*, 2258–2262.